Journal of Clinical Laser Medicine & Surgery
Volume 18, Number 1, 2000
Mary Ann Liebert, Inc.
Pp. 3–8

Fluorescence Spectroscopic Imaging to Detect Changes in Collagen and Elastin Following Laser Tissue Welding

JING TANG, M.D., Ph.D.,[1] FANAN ZENG, B.S.,[1] HOWARD SAVAGE, Ph.D.,[2] PENG PEI HO, Ph.D.,[1] and R.R. ALFANO, Ph.D.[1]

ABSTRACT

***Objective*: A study was performed to evaluate the use of native fluorescence imaging to detect in situ molecular changes. *Summary background data*: There is no ideal noninvasive method to monitor molecular changes in a local region at a laser weld joint without removing a section of tissue for histological examination. *Methods*: Two sections of animal skin were welded together border to border using a Ti:sapphire laser beam (800 nm). Fluorescence imaging was performed on the cross section of the welded site at specific emission wavelengths (λ_e) for collagen at 380 nm and for elastin at 450 nm using excitation wavelengths (λ_e) of 340 nm, and 380 nm, respectively. *Results*: A reduction of the collagen and elastin emission was observed in the fluorescence images of the welded region. These results were confirmed with histology using picrosirius red F3BA under polarized light and orcein stains. *Conclusion*: Optical spectroscopic imaging offers a new noninvasive detecting method for microscopic evaluation of laser tissue welding.**

INTRODUCTION

Laser tissue welding (LTW) is accomplished by directing a laser beam at the opposed edges of two tissue sections being connected. The laser–tissue interaction sealing the tissue may be as effective as suturing. Over the past several years, LTW technology has been shown to: (1) decrease operative time; (2) evade the inherent lithogenic reaction to sutures, clips, and staples; (3) improve wound healing; and (4) provide an immediate intraoperative watertight seal in the repair of many different tissues.[1–4] LTW is a method for connecting tissues that are difficult to suture, such as micrometer to millimeter diameter blood vessels. In addition, LTW is one of the new exciting and promising applications of tissue repair in endoscopic surgery. The mechanism for LTW is still unknown. Several studies have been attempted to understand the process. In 1986, Shober *et al.*[5] studied collagen from rat carotid arteries after Nd:YAG laser welding by electron microscopy. They demonstrated loosening of the collagen triple helix and some sort of interaction between the collagen strands upon laser irradiation. They suggested that welding of the tissue may occur by fusion of the collagen fibers. White, Kopchok and co-workers[6–8] confirmed this concept with argon laser welding of blood vessels. They observed the elastin fibers bound to collagen using electron microscopy.[9] It appears that collagen and elastin fibers play a role in LTW. Tang *et al.*[10] have measured the changes in collagen levels after LTW on blood vessels using biochemical methods. At present, there is no in situ method to detect changes in collagen and elastin levels at a weld joint without removing a section of the tissue. Understanding the changes in the distribution of collagen and elastin simultaneously at a welded site in situ over different periods of time may lead to a better understanding of the mechanism of LTW and improve in vivo human tissue welding.

Fluorescence spectroscopy measures electronic transitions of various photo-excited chromophores in complex tissue structures. There are several natural fluorophores that exist in tissue, which can be excited with ultraviolet light. The fluorescence can be detected in the ultraviolet and visible regions of the spectrum. Collagen and elastin are two important photoactive molecules in tissue.[11] Native fluorescence imaging identifies molecules in tissue samples from the use of different emission and excitation wavelengths. Fluorescence imaging offers a novel noninvasive way to easily detect in situ without removing from

[1]Institute for Ultrafast Spectroscopy and Lasers and New York State Center for Advanced Technology for Ultrafast Photonic Materials and Applications, Departments of Physics and Electrical Engineering, The City College and Graduate School of the City University of New York, New York, New York.
[2]Department of Pathology, New York Eye and Ear Infirmary, New York, New York.

tissue the distribution and quantitative changes in collagen and elastin levels during and after LTW treatment.

This study focuses on using spectral fluorescence imaging to detect in situ the distribution, and changes in collagen and elastin levels after LTW in vitro. The results were confirmed by histology. This work will help understand the underlying mechanism, improve laser tissue welding technology and supply a new method to study LTW.

MATERIALS AND METHODS

The collagen and elastin powders (Sigma, St Louis, MO) were mounted in a 1-mm-thick quartz cuvette, respectively, for spectroscopic study. Spectroscopic measurements were performed using an automated lamp-based spectrophotometer (CD-scan, Mediscience Technology Corp). Fluorescence spectra of collagen and elastin with different excitation wavelengths are shown in Fig. 1a and 1b. The emission wavelength (λ_c) 380 nm with excitation wavelength (λ_e) 340 nm was selected for collagen imaging and $\lambda_c = 450$ nm with $\lambda_e = 380$ nm for elastin imaging.

Laser skin welding was performed using the Ti:sapphire laser (Mira-900F, Coherent Laser Group, Santa Clara CA). It provided a continuous wave laser beam at an 800 nm wavelength. The beam was delivered in a noncontact manner. It was focused with a short focal length lens ($f = 70$ mm) producing a spot size of 0.5 mm, positioned at 50 mm from the lens. The output power out of the focusing lens was 900 mW, measured by a power meter (Scientech 372, Boulder, CO). The corresponding power density was 458 W/cm^2. Under this laser illumination arrangement, the highest tensile strength was achieved after laser skin welding. Details on the use of this method to determine the tensile strength was described in our previous work.[12]

Canine skin samples with a thickness of 2 to 2.5 mm were obtained from the Columbia Presbyterian Hospital, New York. They were harvested from animals being etherized for another study that did not involve the skin tissue. After shaving the fur, the skin sample was cut into a size of 5 mm × 5 mm. Two skin pieces were placed border to border on a translation stage, and free standing. The welding was performed on the region between the two skin pieces by scanning the laser irradiation. The stage was moved forward at approximately 5 mm/30 seconds, then back at the same speed at the same length. A 5 mm fusion line was performed. No conventional suture was performed. The total exposure time was 5 mm/minute. The energy fluence was 27.5 kJ/cm^2.

Once the weld was completed, the skin sample was kept at −20°C for 15 minutes. While the sample was frozen, a cross-section (X-Z plane, see Fig. 2a) through the center of the welded line and perpendicular to X-Y plane was selected for imaging the welded region. Fluorescence imaging and daylight back illuminated photography were performed on the cut cross-section of the joint region of the sample on the X-Z surface (Fig. 2a).

A schematic diagram of the fluorescence spectroscopic imaging setup is shown in Fig. 2b. The light beam from a high-intensity xenon lamp (300 W) was sent through a broad band filter to reduce the heat. It was then transmitted through an optic fiber (excitation fiber). Before exciting the surface of the sample, the light beam passed through a narrow band filter (excitation filter). The central portion of the 10-nm bandwidth light beam was used to illuminate the sample. The fluorescence from the sample was collected by a $f = 105$ mm UV camera lens (lens #1) in the back-scattering geometry. A narrow band filter (emission filter) was inserted at the front of the Lens #1 for fluorescence imaging of the sample. After the signal was amplified by an image intensifier, the fluorescence image was re-imaged with another UV lens (lens #2) onto a CCD camera (TM-72EX, Pulnix America Inc., Sunnyvale, CA). Three pictures per second can be obtained from this imaging system. To improve the signal to noise, each image was averaged over 10 pictures. A personal computer was used to digitize and analyze the image. The controlling software generated and displayed the fluorescence maps.

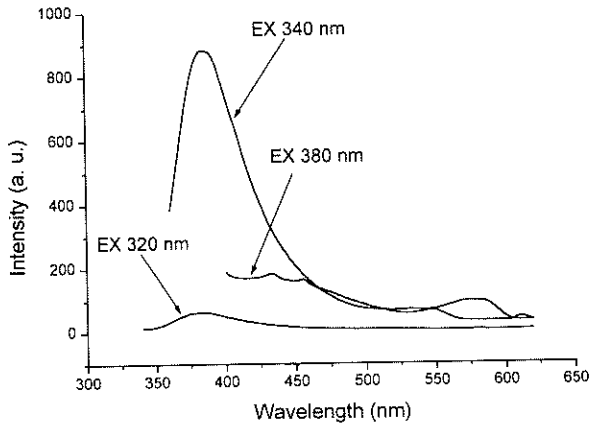

(a)

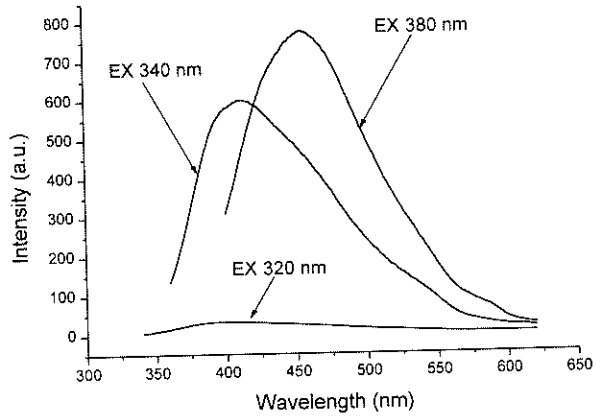

(b)

FIG. 1. **a:** The fluorescence spectra of collagen excited by different wavelengths. To obtain the optimum fluorescent intensity, the 380 nm signal under 340 nm excitation is selected to probe collagen. **b:** The fluorescence spectra of elastin excited by different wavelengths. To obtain the optimum fluorescent intensity, the 450 nm signal under 380 nm excitation is selected to probe elastin.

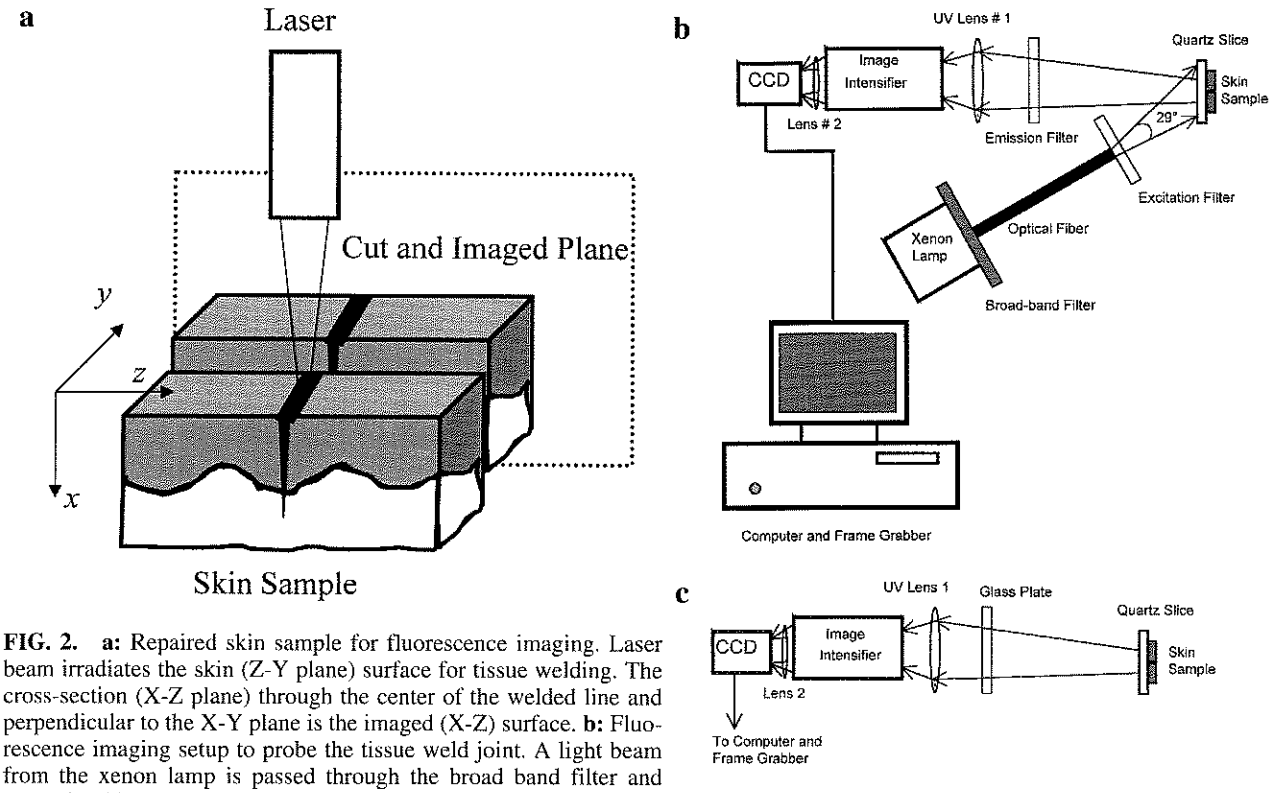

FIG. 2. **a:** Repaired skin sample for fluorescence imaging. Laser beam irradiates the skin (Z-Y plane) surface for tissue welding. The cross-section (X-Z plane) through the center of the welded line and perpendicular to the X-Y plane is the imaged (X-Z) surface. **b:** Fluorescence imaging setup to probe the tissue weld joint. A light beam from the xenon lamp is passed through the broad band filter and transmitted by the optical fiber to excite sample surface. The emitted beam is passed through a narrow band excitation filter (340 nm for collagen imaging, and 380 nm for elastin imaging). The fluorescence from the sample is collected by UV lens #1 and imaged onto an image intensifier. The emission filter at 380 nm selects the collagen signal, and at 450 nm selects the elastin signal and is inserted at the front of the UV lens #1. The signals are amplified by the image intensifier. The intensified fluorescence image is then imaged by lens #2 onto the CCD camera. A personal computer is used to digitize, display, and analyze the image profiles. **c:** Back-illuminated photography setup. The glass plate is placed at the front of the UV lens #1 instead of the emission filter to obtain the same focus and size image as for fluorescence imaging. The sample is illuminated with room daylight.

The setup used for back illuminated photography of the joint is shown in Fig. 2c. A glass plate was placed in front of lens #1 instead of the emission filter to obtain the same focus and image size as in fluorescence imaging. The sample was illuminated with room lights.

After obtaining native fluorescence and back imaging, the tissue samples were fixed in 10% phosphate-buffered formalin. The tissues were dehydrated in graded ethanol solution and xylene and embedded in paraffin. Each of the lesions was sectioned at 5 μm. Sections from the lesion were stained with Gill's hematoxylin eosin, picrosirius red F3BA, and Orcein stains. The specimen stained with picrosirius red F3BA was observed with a polarizing microscope (Reichert, Vienna, Austria). The other specimens were observed with a normal optical microscope (Vanox-T, Olympus, Japan). Both microscopes were equipped with a color video camera with 3 CCD chips (DXC-97 MD, Sony, Japan) for obtaining histology images.

RESULTS

The laser-irradiated skin region showed slight tissue ablation in the surface of the welded tissue and a slight discoloration and translucence at the fusion line on the cross section. The average initial post-welded tensile strength value was measured to be 0.30 ± 0.12 N ($n = 10$).

Figure 3 shows the cross sections of daylight back-illuminated photograph and fluorescence image. Densitometry correspondent Fig. 3 is made in Fig. 4 to show the changes in fluorescence intensity at different regions more clearly. The correspondent densitometry curve 1 to 4 is obtained from the traces shown in Fig. 4d. The daylight back illuminated photograph of the LTW region is shown in Fig. 3a. The correspondent densitometry at different depths from the skin surface to the subcutaneous layer is shown in Fig. 4a. The ablated region on the surface of the skin sample and the welded line below are visible, but the extent of adjacent thermal treatment is not evident. The image at $\lambda_c = 380$ nm with $\lambda_e = 340$ nm for collagen imaging is shown in Fig. 3b. The densitometry at different depths from the skin surface to the subcutaneous layer is shown in Fig. 4b. Due to the collagen denatured by laser heating and the consequent loss of fluorescence, the welded site becomes a fluorescence void, and appears as a crater, in which the depth from the skin surface to the deepest point is 1.6 ± 0.65 mm ($n = 10$). The image at $\lambda_c = 450$ nm with $\lambda_e = 380$ nm for elastin imaging is shown in Fig. 3c. The correspondent densitometry at different depths from the skin surface to the subcutaneous layer is shown in Fig. 4c. The crater is also evident, due

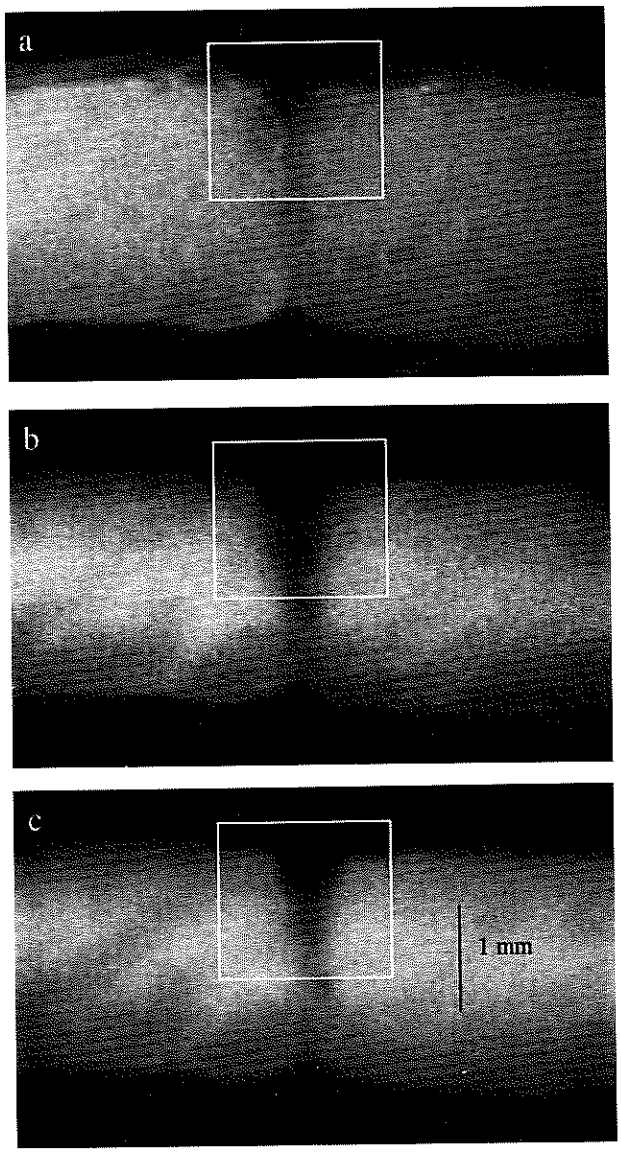

FIG. 3. Cross-section images of welded skin tissue show the welded joint in the white square. **a:** Daylight back-illuminated photograph; the extent of thermal treatment is not evident. **b:** Collagen imaging; due to collagen being denatured by laser heating and the resultant loss of its fluorescence, the welded site appears as a crater. **c:** Elastin imaging; due to denatured elastin, the welded site appears as a crater. ×18.

to the denaturation of elastin. The size of the crater for elastin (Fig. 3c) is less than that of collagen (Fig. 3b). A depth of 1.2 ± 0.72 mm (n = 10) is measured. In both the collagen and elastin images (Fig. 3b and 3c) and densitometries (Fig. 4b and 4c), the epidermal layer, dermal layer, and subcutaneous layer of the skin samples can be identified by the different fluorescence intensities. The dermal layer is clearer than the epidermal and subcutaneous layers in the fluorescence image (Fig. 3) and more intense in densitometry (Fig. 4). The crater depth and size in collagen imaging (Fig. 4b) are quite similar to the thermal damage depth and size in the histological result with the picrosirius red F3BA stain observed under polarized light (Fig.

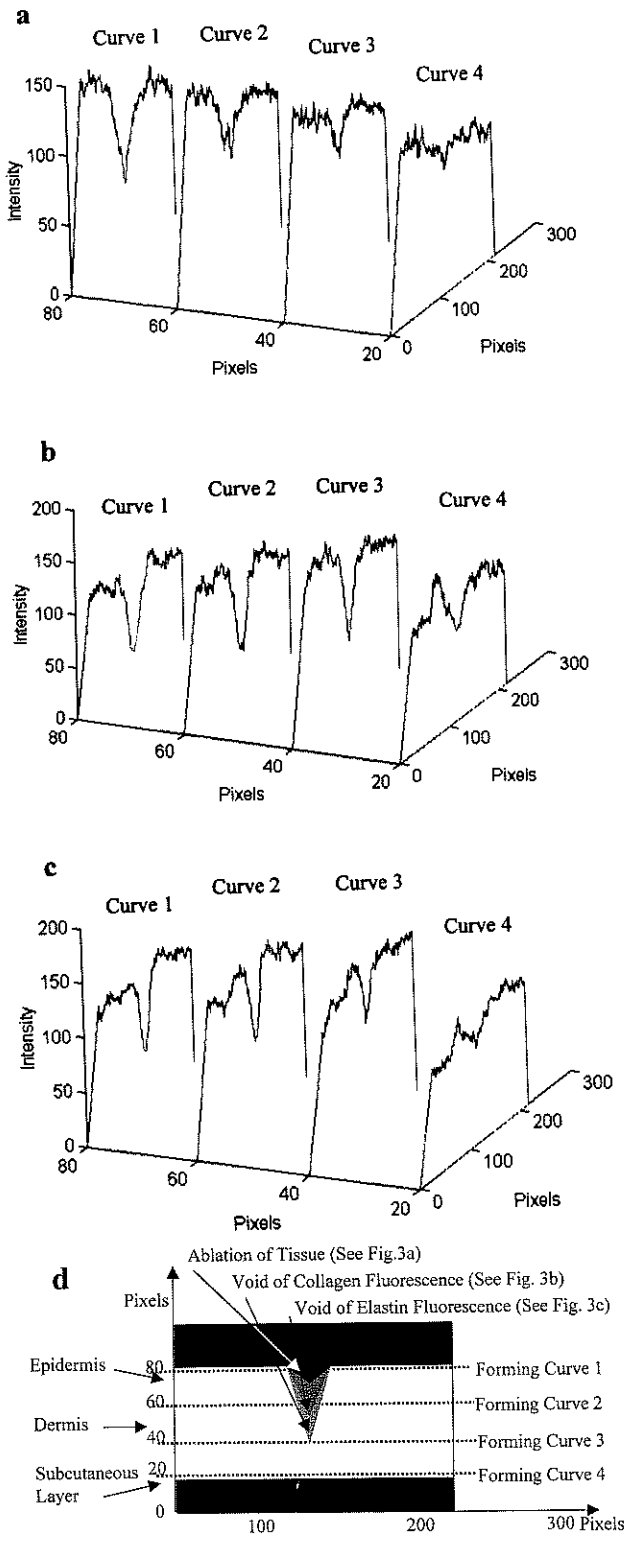

FIG. 4. Digital fluorescence intensity distribution of the region highlight in Fig. 3. Four rows are selected (**d**) Densitometry at different depths from the skin surface to subcutaneous layer identifies the fluorescence intensity at epidermal, dermal, and subcutaneous layers. **a:** From the daylight back illuminated photograph in Fig. 3a. **b:** From the collagen imaging in Fig. 3b. **c:** From the elastin imaging in Fig. 3c. Note the craters due to the lack of collagen or elastin emission and the higher intensity in curve 2 and curve 3 due to richer collagen or elastin on the dermal layer in b and c.

5b). A depth of 1.3 ± 0.72 mm (n = 9) is measured from the microscopic slides, after a tissue-shrinkage multiplicative correction factor of 1.15 is used.[13,14] The image at λ_c = 450 nm with λ_e = 380 nm for elastin imaging (Fig. 4c) and is quite similar to the histological result, which is colored with orcein stain (Fig. 6).

DISCUSSION

In fluorescence imaging at selected emission and excitation wavelengths, the size and depth of collagen or elastin loss in the cross section can be directly observed, due to collagen or elastin denaturing by laser heating and consequent loss in their fluorescence. Denaturation of collagen occurs approximately at 65°C.[15] Since elastin is more resistant to denaturation (by heating),[16] the crater is less in the elastin image than in the collagen image.

The densitometry (Fig. 4) obtained from the fluorescence image (Fig. 3) is useful to identify the changes in the fluorescence intensity at the welded site after laser tissue welding. The densitometry at different depths from the skin surface to the subcutaneous layer also can show that there are different fluorescence intensities in epidermal, dermal, and subcutaneous layers. The fluorescence intensity of collagen and elastin in the dermal layer is more than in the epidermal and subcutaneous layers. The histology also confirms these results.

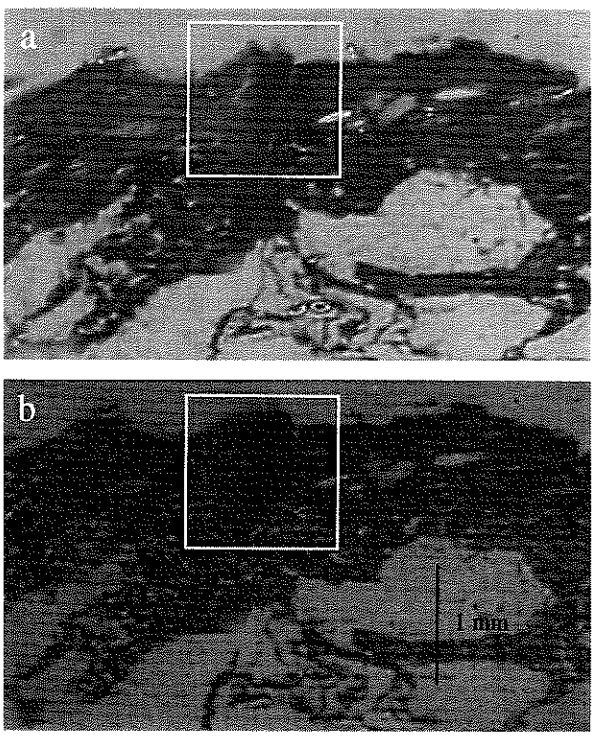

FIG. 5. Histological cross sections of skin tissue after laser welding show the welded joint in the white square. **a:** Section is stained using picrosirius red F3BA without polarized light. The tissue structure at the welded joint disappears and become homogenized. The junction between normal and denatured collagen fibers can not be identified. **b:** In the same slide under polarized light, stained collagen fibers appear yellow/orange. Due to collagen denaturing and the loss of its natural birefringence, the welded site can not be seen in stained collagen fibers. The welded joint appears as a crater. ×18.

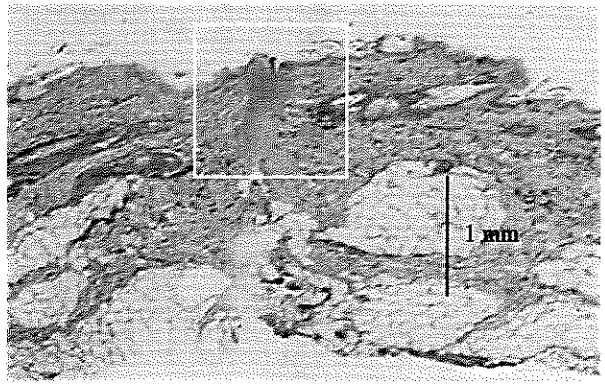

FIG. 6. Cross section of skin tissue after welding by histology. The section is stained with orcein stain. After this special stain, elastin fibers became black interspersed, as small and short sticks, in the skin tissue. Due to elastin denaturation, the welded site shown in the white square can not be display stained elastin fibers. ×18.

The histology using picrosirius red F3BA stain illuminated by polarized light is described as a specific stain for collagen molecules in a variety of tissues. The sulfonic acid groups of the dye react with the basic groups on the collagen molecule; the natural birefringence of collagen is then enhanced by the parallel relationship of the elongated dye molecules.[17] However, thermally denatured collagen does not exhibit this birefringence. Collagen denaturation can therefore be used as a marker for thermal damage.[18] Picrosirius red F3BA with polarized light has been used to examine the effect of laser energy on the collagen of vascular tissue[18,19] and to criticize quantitative and comparative means of assessing collagen thermal damage resulting from laser techniques.[18,20] Orcein stain is a classical histology examination for elastin fiber.

The use of native fluorescence of tissue allows for imaging molecular components LTW. Fluorescence imaging may develop a wide range of noninvasive diagnostic tools for in vivo and in vitro welded tissue examination. In this study using canine skin tissue, we confirm that collagen and elastin fibers in the welded site are denatured after laser irradiation. The denatured collagen and elastin lose their native fluorescence.

The quantitative measurement of collagen and elastin in tissue in situ may be possible. The quantitative changes in collagen and elastin after LTW at different periods will be performed in a future study.

ACKNOWLEDGMENTS

This work is supported in part by the DOE Center of Excellence Program. The authors thank Dr. B. Xu for operating the Ti:sapphire laser and Dr. N. Ockman for reviewing the text.

REFERENCES

1. Bass, L.S. (1995). Laser tissue welding: a comprehensive review of current and future clinical applications. Lasers Surg. Med. 17, 315–349.
2. Poppas, D.P., Choma, T.J., Rooke, C.T., Klioze, S.D., and Schlossberg, S.M. (1993). Preparation of human albumin solder for laser tissue welding. Lasers Surg. Med. 13, 577–580.
3. Tang, J., Godlewski, G., Rouy, S., Dauzat, M., Juan, J.M., Chambettaz, F., Delacretaz, G., and Salathe, R.P. (1994). Microarterial anastomosis using a non contact diode laser versus a control study. Lasers Surg. Med. 14, 229–237.
4. Tang, J., Godlewski, G., Rouy, S., Prudhomme, M., Delacretaz, G., and Salathe, R.P. (1997). Morphological analysis of the microarterial media repair after 830 nm diode laser assisted end-to-end anastomosis, comparison with conventional manual suture. Laser Med. Sci. 12, 300–308.
5. Schober, R., Ulirich, F., Sander, T., Durselen, H., and Hessel, S. (1986). Laser-induced alteration of collagen substructure allows microsurgical tissue welding. Science 232, 1421–1422.
6. White, R.A., Kopchok, G.E., Donayre, C.E., Peng, S.K., Fujitani, R.M., White, G.H., and Uitto, J. (1988). Mechanism of tissue fusion in argon laser-welded vein-artery anastomoses. Lasers Surg. Med. 8, 83–89.
7. Kopchok, G.E., White, R.A., White, G.H., Fujitani, R.M., Vlasak, J., Dykhovsky, L., and Grundfest, W. (1988). CO_2 and argon laser vascular welding: acute histological and thermodynamic comparison. Lasers Surg. Med. 8, 584–588.
8. Kopchok, G.E., White, R.A., Grundrest, W.S., Fujitani, R.M., Klein, S.R., and White, G.H. (1988). Thermal studies of in-vivo vascular tissue fusion by argon laser. J. Invest. Surg. 1, 5–12.
9. White, R.A., White, G.H., Fujitani, R.M., Vlasak, J.W., Donayre, C.E., Kopchok, G.E., and Peng, S.K. (1989). Initial human evaluation of argon laser-assisted vascular anastomoses. J. Vasc. Surg. 9, 542–547.
10. Tang, J., O'Callaghen, D., Rouy, S., Godlewski, G., and Prudhomme, M. (1998). Quantitative changes in collagen levels following diode laser welding. Lasers Surg. Med. 22, 207–211.
11. Alfano, R.R., and Katz, A. (1996). Photonic pathology, fluorescence and Raman spectroscopy for tissue diagnosis and characterization. Analytical use of fluorescent probes in oncology. New York: Plenum, pp. 81–89.
12. Tang, J., Evans, M., Petričviće, P., Ho, P.P., and Alfano, R.R. (1999). Tissue welding using Near-infrared forsterite and cunyite tunable lasers. IEEE J. STQE 5, 1103–1106.
13. Boonstra, H., Oosterhuis, J.W., Oosterhuis, A.M., and Fleuren, G.J. (1983). Cervical tissue shrinkage by formaldehyde fixation, paraffin wax embedding, section cutting and mounting. Virchows Arch. A Pathol. Anat. Histopathol. 402, 195–201.
14. Schned, A.R., Wheeler, K.J., Hodorowski, C.A., Heaney, J.A., Ernstoff, M.S., Amdur, R.J., and Harris, R.D. (1996). Tissue-shrinkage correction factor in the calculation of prostate cancer volume. Am. J. Surg. Pathol. 20, 1501–1506.
15. Lelous, M., Flandin, F., Herbage, D., and Allain, J-C. (1982). Influence of collagen denaturation on the chemorheological properties of skin assessed by differential scanning calorimetry and hydrothermal isometric tension measurements. Biochem. Biophys. Acta 717, 295–300.
16. Rucker, R.B., and Tinker, D. (1977). In *Encylopedia of Human Biology*, 2nd ed., Vol. 3, Dulbecco R (ed.) New York: Academic Press, pp. 573–582.
17. Boulnois, J-L. (1985). Photophysical processes in recent medical laser developments: a review. Lasers Surg. Med. 1, 47–66.
18. Brooks, S.G., Ashley, S., Wright, S., Davies, G.A., Kester, R.C., and Rees, M.R. (1991). The histological measurement of laser-induced thermal damage in vascular tissue using the stain picrosirius red F3BA. Lasers Med. Sci. 6, 399–405.
19. Macruz, R., Ribeiro, M.P., and Brum, J.M.C. (1985). Laser surgery in enclosed spaces: a review. Lasers Surg. Med. 5, 199–218.
20. Prudhomme, M., Rouy, S., Tang, J., Landgrebe, J., Delacretaz, G., and Godlewski, G. (1999). Biliary structures lead to tumour recurrences after laser-induced interstitial thermotherapy. Lasers Surg. Med. 6, 399–405.

Address reprint requests to:
R.R. Alfano, Ph.D.
Institute for Ultrafast Spectroscopy and Lasers
Department of Physics
The City College of the City University of New York
138th Street and Convent Avenue
New York, NY 10031

E-mail: alfano@scisun.sci.ccny.cuny.edu